

[10]-Gingerdiols as the Major Metabolites of [10]-Gingerol in Zebrafish Embryos and in Humans and Their Hematopoietic Effects in Zebrafish Embryos

Huadong Chen,[†] Dominique N. Soroka,[†] Jamil Haider,[‡] Karine F. Ferri-Lagneau,[‡] TinChung Leung,[‡] and Shengmin Sang^{*,†}

[†]Center for Excellence in Post-Harvest Technologies, North Carolina Agricultural and Technical State University, North Carolina Research Campus, 500 Laureate Way, Kannapolis, North Carolina 28081, United States

[‡]Nutrition Research Program, Julius L. Chambers Biomedical/Biotechnology Research Institute, North Carolina Central University, North Carolina Research Campus, 500 Laureate Way, Kannapolis, North Carolina 28081, United States

ABSTRACT: Gingerols are a series of major constituents in fresh ginger with the most abundant being [6]-, [8]-, and [10]-gingerols (6G, 8G, and 10G). We previously found that ginger extract and its purified components, especially 10G, potentially stimulate both the primitive and definitive waves of hematopoiesis (blood cell formation) in zebrafish embryos. However, it is still unclear if the metabolites of 10G retain the efficacy of the parent compound toward pathological anemia treatment. In the present study, we first investigated the metabolism of 10G in zebrafish embryos and then explored the biotransformation of 10G in humans. Our results show that 10G was extensively metabolized in both zebrafish embryos and humans, in which two major metabolites, (3S,5S)-[10]-gingerdiol and (3R,5S)-[10]-gingerdiol, were identified by analysis of the MSⁿ spectra and comparison to authentic standards that we synthesized. After 24 h of treatment of zebrafish embryos, 10G was mostly converted to its metabolites. Our results clearly indicate that the reductive pathway is a major metabolic route for 10G in both zebrafish embryos and humans. Furthermore, we investigated the hematopoietic effect of 10G and its two metabolites, which show similar hematopoietic effects as 10G in zebrafish embryos.

KEYWORDS: [10]-gingerol, metabolism, hematopoiesis, zebrafish embryos, human urine

■ INTRODUCTION

Ginger, the rhizome of *Zingiber officinale*, has been used worldwide not only as a spice but also as a useful crude drug in traditional Chinese medicine. Recently, there has been a surfeit of scientific research to validate the use of ginger for symptoms such as inflammation, cancer, nausea and vomiting during pregnancy, sprains, muscular aches, cramps, constipation, hypertension, fever, and infectious diseases, as well as rheumatic and gastrointestinal effects.^{1,2} The fresh rhizome of ginger contains a rich source of biologically active constituents including volatile oils (1% to 3%) and nonvolatile pungent oleoresin components.³ A variety of active components were identified in the oleoresin of ginger including gingerols, a series of homologues with varied unbranched alkyl chain lengths with the most abundant being [6]-, [8]-, and [10]-gingerol (6G, 8G, and 10G, respectively)^{4–6} (Figure 1).

Gingerols have been found to possess many distinct pharmacological and physiological activities. For example, [6]-gingerol has been reported to significantly and dose-dependently restore renal functions, reduce lipid peroxidation, and enhance the levels of reduced glutathione and activities of superoxide dismutase and catalase against cisplatin-induced oxidative stress and renal dysfunction in rats.⁷ With our collaborators, we have found that [6]-gingerol was more effective than curcumin, a known cancer preventive agent from *Curcuma longa* L., in inhibiting 12-*O*-tetradecanoylphorbol 13-acetate (TPA)-induced tumor promotion in mice.⁸ Although many reports demonstrate similar bioactivities among different

gingerols, varying side chain lengths of gingerols may influence their biological efficacies. For example, [10]-gingerol displayed stronger quenching ability of DPPH radicals than [6]-gingerol, [6]-shogaol, and curcumin in a study comparing activities of twenty-nine phenolic compounds isolated from root bark of fresh ginger.⁹ In the same study, [10]-gingerol exhibited higher inhibition of lipid peroxidation of rat brain homogenates than quercetin.⁹ Earlier research on isolated components of dried rhizomes of ginger showed that [10]-gingerol exhibited higher toxicity than [4]-, [6]-, and [8]-gingerols against human A549, SK-OV-2, SK-MEL-2, and HCT15 tumor cells.¹⁰ In particular, we studied the hematopoiesis promoting effects of ginger extract and its components [6]-, [8]-, and [10]-gingerol, and [6]-, [8]-, and [10]-shogaol in zebrafish embryos, in which 10G showed higher activities among these gingerols and shogaols. We also demonstrated that treatment with 10G promoted hematopoietic recovery from phenylhydrazine-induced anemia in zebrafish embryos,¹¹ while the efficacy of its metabolites is still unknown.

The pharmacokinetics of [10]-gingerol have been examined in humans and in rats.^{3,12–14} For example, Zick et al. reported that, 1 h after oral administration of 2.0 g of ginger extracts (containing 24.4 mg of 10G), free 10G and its glucuronidated

Received: April 4, 2013

Revised: May 13, 2013

Accepted: May 14, 2013

Published: May 14, 2013

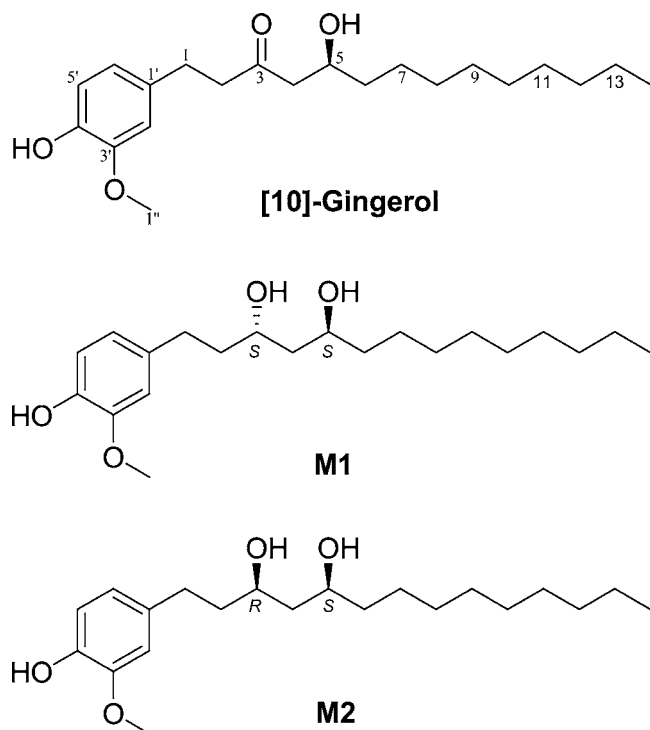


Figure 1. Chemical structures of [10]-gingerol and its major metabolites M1 and M2.

and sulfated metabolites were detected in human plasma with peak concentrations of 9.5 ± 2.2 ng/mL, 370 ± 190 ng/mL, and 18.0 ± 6.0 ng/mL, respectively, and very low concentrations (2–3 ng/mL) of 10G glucuronide and sulfate were found in human colon tissues.¹² This study concluded that the only nonconjugated ginger components detected in the plasma were 10G and [6]-shogaol, thereby warranting further validation of the pharmacological efficacy of these compounds.¹² Additionally, Wang et al. reported that only free 10G was detected in plasma of rats up to four hours after oral administration of 300 mg/kg ginger oleoresin, with no detectable glucuronide or sulfate conjugates between zero and seven hour harvests.¹³

Given the short apparent half-life of [10]-gingerol, studies of its biotransformation are necessary. However, limited data have been reported on the metabolism of 10G, which may influence its bioactivity in vivo. Furthermore, significant differences in metabolic pathways among different species may exist. The various metabolites and their concentrations can potentially affect in vivo bioactivities and toxicities. For example, coumarin is metabolized to 7-hydroxy coumarin in human and in mouse. However, in the surrogate rat model, coumarin is transformed to a carcinogenic epoxide, a drastic consequence of differential metabolism in seemingly similar mammals.¹⁵ This proven rationale of interspecies variation in terms of metabolic behavior was part of the impetus to investigate the biotransformation of 10G in both zebrafish embryos and humans. As our previous study showed, 10G positively promotes hematopoiesis (blood cell formation) in zebrafish embryos.¹¹ The current study therefore investigates the metabolism of 10G in zebrafish embryos and in humans to compare its biotransformation in these two models, and examines the hematopoietic effects of the metabolites of [10]-gingerol.

MATERIALS AND METHODS

Materials. 10G was purified from ginger extract in our laboratory.¹⁶ Analytical TLC plates, dimethyl sulfoxide (DMSO), and CDCl_3 were purchased from Sigma (St. Louis, MO). HPLC-grade solvents and other reagents were obtained from VWR Scientific (South Plainfield, NJ). HPLC-grade water was prepared using a Barnstead Nanopure water purification system (Waltham, MA). Liquid chromatography/mass spectrometry (LC/MS)-grade water and MeOH were obtained from Thermo Fisher Scientific (Waltham, MA). Ginger tea bags for human experiment were bought from the local supermarket, and the level of [10]-gingerol was 4.66 mg/100 g according to our previous reports.¹⁷

Biotransformation of 10G in Zebrafish Embryos. Zebrafish embryos were staged and maintained according to NCCU IACUC guidelines. In general, fifty zebrafish embryos at the 10–11 h postfertilization (hpf) stage were incubated at 28.5 °C in 0.3× Danieau's solution (19.3 mM NaCl, 0.23 mM KCl, 0.13 mM MgSO_4 , 0.2 mM $\text{Ca}(\text{NO}_3)_2$, 1.7 mM HEPES, pH 7.0) with or without 5 $\mu\text{g}/\text{mL}$ 10G. At 24 hpf, embryos were dechorionated manually and the chorions were carefully removed one by one from the culture medium, so that we did not significantly change the volumes of the solutions. At 28–30 hpf, zebrafish embryos were harvested for analysis.

Zebrafish Embryo Sample Preparation. Acetonitrile (300 μL) with 0.2% acetic acid was added to 50 zebrafish embryos. Samples were homogenized for 90 s by an Omni Bead Ruptor Homogenizer (Kennesaw, GA) and then centrifuged at 17000g for 10 min. The supernatant (250 μL) was collected and diluted 5 times for HPLC and LC–MS analysis.

Synthesis of the Two Major Metabolites of 10G. NaBH_4 (57 mg, 1.5 mmol) was added to a solution of 10G (210 mg, 0.6 mmol) in methanol at 0 °C. After stirring at 0 °C for 2 h, the reaction medium was neutralized with a diluted acetic acid solution (0.1 M) and extracted with ethyl acetate (10 mL \times 3). Combined organic layers were concentrated under reduced pressure. The residue was purified by preparative HPLC to produce the required compounds M1 (44 mg) and M2 (84 mg).

Separation of the Isomers (M1 and M2) Using Preparative HPLC. Waters preparative HPLC systems with 2545 binary gradient module, Waters 2767 sample manager, Waters 2487 autopurification flow cell, Waters fraction collector III, dual injector module, and 2489 UV/visible detector were used to separate M1 and M2. A Phenomenex Gemini-NX C_{18} column (250 mm \times 30.0 mm i.d., 5 μm) was used with a flow rate of 20.0 mL/min. The wavelength of the UV detector was set at 230 nm. The injection volume was 0.5 mL for each run. The mobile phase consisted of solvent A (H_2O) and solvent B (MeOH). The mixtures of M1 and M2 were injected to the preparative column and eluted with an isocratic elution (80% B) for 20 min. M1 and M2 were eluted at 16.5 and 16.8 min, respectively.

Human Urine Samples. The Institutional Review Board approved the protocol for human experimentation through the Protection of Human Subjects in Research (11-0092) at North Carolina Agricultural & Technical State University. Three healthy male volunteers (30–40 years old, weighing 60–80 kg, nonsmokers) participated in the study. The subjects did not consume ginger or ginger products for at least 3 days before the experiment. They had the same breakfast, lunch, and dinner during the experiment. The first urine sample was collected just before breakfast, which included 200 mL of two reconstituted ginger tea bags (18 g/bag), and the rest were at 0–2, 2–4, 4–6, 6–9, 9–12, and 12–24 h thereafter. The urine samples were stored at -80 °C before analysis.

Human Urine Sample Preparation. Enzymatic deconjugation was performed as described previously with slight modification.¹⁸ In brief, duplicate human urine samples were prepared in the presence of β -glucuronidase (250 U) and sulfatase (3 U) for 24 h at 37 °C and then extracted twice with ethyl acetate. The ethyl acetate fraction was dried under vacuum, and the solid was resuspended in 200 μL of 80% aqueous methanol with 0.1% acetic acid for further LC/MS analysis.

HPLC Analysis. An HPLC-ECD (ESA, Chelmsford, MA) consisting of an ESA model 584 HPLC pump, an ESA model 542

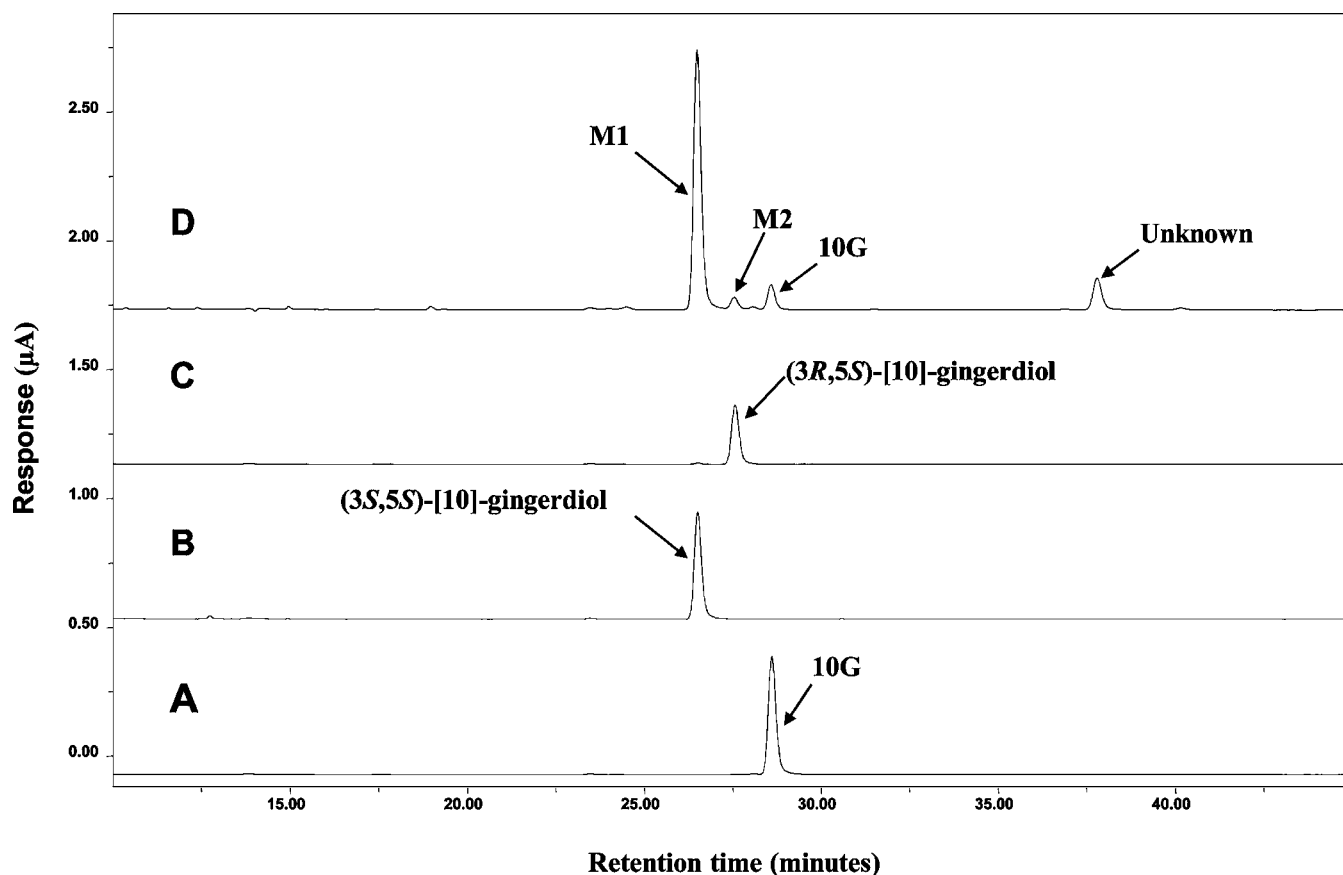


Figure 2. HPLC-ECD chromatograms of [10]-gingerol (10G) (A), (3*S*,5*S*)-[10]-gingerdiol (B), and (3*R*,5*S*)-[10]-gingerdiol (C) standards, and lysate of 10G treated zebrafish embryos (D).

autosampler, an ESA organizer, and an ESA CoulArray detector coupled with two ESA model 6210 four sensor cells, was used in our study. A Gemini C_{18} column (150 mm \times 4.6 mm, 5 μ m; Phenomenex, Torrance, CA) was used for chromatographic analysis at a flow rate of 1.0 mL/min. The mobile phases consisted of solvent A (30 mM sodium phosphate buffer containing 1.75% acetonitrile and 0.125% tetrahydrofuran, pH 3.35) and solvent B (15 mM sodium phosphate buffer containing 58.5% acetonitrile and 12.5% tetrahydrofuran, pH 3.45). The gradient elution had the following profile: 20% B from 0 to 3 min; 20–55% B from 3 to 11 min; 55–60% B from 11 to 12 min; 60–65% B from 12 to 13 min; 65–100% B from 13 to 40 min; 100% B from 40 to 45 min; and 20% B from 45.1 to 50 min. The cells were then cleaned at a potential of 1000 mV for 1 min. The injection volume of the sample was 10 μ L. The eluent was monitored by the Coulochem electrode array system (CEAS) with potential settings at 200, 250, 300, 350, 400, 450, and 500 mV. Data for Figure 2 was from the channel set at 350 mV of the CEAS.

LC/APCI-MS Method. LC/MS analysis was carried out with a Thermo-Finnigan Spectra System, which consisted of an Accela high-speed MS pump, an Accela refrigerated autosampler, and an LTQ Velos ion trap mass detector (Thermo Electron, San Jose, CA) incorporated with atmospheric-pressure chemical ionization (APCI) interfaces. A Gemini C_{18} column (150 \times 4.6 mm i.d., 5 μ m; Phenomenex, Torrance, CA) was used for separation at a flow rate of 0.7 mL/min. The column was eluted with 100% solvent A (5% aqueous methanol with 0.2% acetic acid) for 1 min, followed by linear increases in B (95% aqueous methanol with 0.2% acetic acid) to 50% from 1 to 5 min, to 85% from 5 to 10 min, isocratic elution with 85% for 15 min, then to 100% from 25 to 33 min, and then with 100% B from 33 to 40 min. The column was then re-equilibrated with 100% A for 5 min. The LC eluent was introduced into the APCI interface. The positive ion polarity mode was set for the APCI source with the voltage on the APCI interface maintained at approximately 4.5 kV.

Nitrogen gas was used as the sheath gas and auxiliary gas. Optimized source parameters, including APCI capillary temperature (330 $^{\circ}$ C), vaporizer temperature (400 $^{\circ}$ C), sheath gas flow rate (45 units), auxiliary gas flow rate (20 units), and tube lens (50 V), were tuned using authentic 10G. The collision-induced dissociation (CID) was conducted with an isolation width of 2 Da and normalized collision energy of 35 for MS^2 and MS^3 . Default automated gain control target ion values were used for $MS-MS^3$ analyses. The mass range was measured from 100 to 1000 m/z . Data acquisition was performed with Xcalibur version 2.0 (Thermo Electron, San Jose, CA, USA).

Nuclear Magnetic Resonance (NMR) Analysis. 1H , ^{13}C , and two-dimensional (2D) spectra were acquired on a Bucker AVANCE 600 MHz instrument (Bruker, Inc., Silberstreifen, Rheinstetten, Germany). All compounds were analyzed in $CDCl_3$. 1H and ^{13}C NMR data of 10G, M1, and M2 are listed in Table 1.

Hematopoietic Effects of 10G and Its Metabolites (M1 and M2) in Zebrafish Embryos. *Transgenic Zebrafish and Embryos.* Zebrafish (*Danio rerio*) AB transgenic strains *Tg(gata1:dsRed)*¹⁹ were maintained in an Aquaneering fish housing system with 14 h light/10 h dark cycle. The fish embryos were maintained at 28.5 $^{\circ}$ C in 0.3 \times Danieau's solution (19.3 mM NaCl, 0.23 mM KCl, 0.13 mM $MgSO_4$, 0.2 mM $Ca(NO_3)_2$, 1.7 mM HEPES, pH 7.0) containing 30 μ g/mL phenylthiourea (PTU) to inhibit pigmentation. Zebrafish embryos were washed, dechorionated, and anesthetized before observations and fluorescence video imaging for analysis.

Fluorescent Microscopy. Olympus MVX10 MacroView fluorescence microscope (Olympus, Center Valley, PA) equipped with Hamamatsu C9300-221 high-speed digital CCD camera (Hamamatsu City, Japan) were used for fluorescence video microscopy. *Tg(gata1:dsRed)* fluorescent embryos were anesthetized in tricaine (0.168 mg/mL) and imaged at 5 dpf (days postfertilization). MetaMorph TL for Olympus software (Olympus, Center Valley, PA) was used for image acquisition and analysis.

Table 1. δ_{H} (600 MHz) and δ_{C} (150 MHz) NMR Spectral Data of 10G, M1, and M2 (CDCl_3 , δ in ppm and J in Hz)

	10G		M1		M2	
	δ_{H} multi (J)	δ_{C}	δ_{H} multi (J)	δ_{C}	δ_{H} multi (J)	δ_{C}
1	2.63 m 2.73 m	31.88	2.51 m 2.62 m	31.94 a ^a	2.52 m 2.61 m	31.38
2	2.63 m 2.73 m	45.43	1.65 m 1.74 m	39.37	1.65 m 1.74 m	39.98
3		211.48	3.88 m	68.96	3.80 m	72.46
4	2.39 dd (9.1, 17.4) 2.46 dd (2.7, 17.4)	49.35	1.54 m	42.37	1.48 m	42.75
5	3.92 m	67.68	3.86 m	69.61	3.76 m	73.43
6	1.30 m 1.40 m	36.47	1.36 m 1.43 m	37.51	1.36 m	38.27
7	1.16 m 1.30 m	25.45	1.19 m 1.32 m	25.77	1.19 m 1.29 m	25.32
8	1.16 m	29.57 a	1.18 m	29.62 b	1.18 m	29.59 a
9	1.16 m	29.54 a	1.18 m	29.61 b	1.18 m	29.59 a
10	1.16 m	29.54 a	1.18 m	29.56 b	1.18 m	29.55 a
11	1.16 m	29.30 a	1.18 m	29.31 b	1.18 m	29.31 a
12	1.16 m	29.27 a	1.17 m	31.89 a	1.17 m	31.88
13	1.16 m	22.67	1.19 m	22.68	1.19 m	22.67
14	0.78 t (7.0)	14.11	0.78 t (7.0)	14.11	0.78 t (7.0)	14.11
1'		132.64		133.90		133.85
2'	6.58 s	111.00	6.61 s	111.01	6.62 s	111.05
3'		146.46		146.46		146.45
4'		143.97		143.73		143.72
5'	6.72 d (8.0)	114.40	6.73 d (8.0)	114.31	6.73 d (8.0)	114.29
6'	6.56 d (8.0)	120.73	6.59 d (8.0)	120.86	6.59 d (8.0)	120.88
OMe	3.77 s	55.87	3.77 s	55.87	3.77 s	55.87

^aThe same letter a or b indicates that the assignments are interchangeable.

Comparison of Erythropoiesis-Stimulating Activity for 10G and Metabolites. The effects of 10G and its metabolites were compared by their abilities to increase the production of erythrocytes during recovery in an acute hemolytic anemia zebrafish model.¹¹ Phenylhydrazine (PHZ) (0.7 $\mu\text{g}/\text{mL}$) was added into 0.3 \times Danieau's embryo medium at 28 hpf. The PHZ was washed 3 times extensively with embryo medium at 48 hpf. Then, embryos were incubated with 10G or metabolites (1.0 $\mu\text{g}/\text{mL}$). On day 5 (5 dpf), embryos were anesthetized and fluorescent erythrocytes from the transgenic *Tg(gata1:dsRed)* embryos were imaged at the dorsal aorta of the tail region (see the box of the cartoon in Figure 5a). Videos of circulating erythrocytes within the dorsal aorta were analyzed with about 24–30 embryos per group by counting the number of *Tg(gata1:dsRed)* fluorescent cells entering/exiting the video (100 frames in 1 s; 327 μm distance). The relative number of erythrocytes was normalized by the measured blood flow. Data are presented as mean \pm SEM. p values were determined by using Student's t test. $p < 0.01$ was considered statistically significant. One-way ANOVA was used to determine the difference among groups.

RESULTS

Synthesis and Structure Elucidation of the Metabolites of 10G in Zebrafish Embryos. After 18–19 h incubation of 10G with zebrafish embryos, three major metabolites (M1, M2, and one unknown) were detected by HPLC chromatography (Figure 2). Previously, we reported that [6]-gingerol was metabolized to two major metabolites, isomeric [6]-gingerdiols.²⁰ Since 10G and 6G are different only in side chain length, we speculated that they shared a similar biotransformation pathway. 10G was reduced by NaBH_4 and separated by preparative HPLC (as described in Materials and Methods) to give two products. Their structures were established by analyzing the ^1H , ^{13}C , and 2D NMR (HMQC

and HMBC) spectra as well as by comparing with literature data.²¹ One product showed the molecular formula $\text{C}_{21}\text{H}_{36}\text{O}_4$ based on positive APCI-MS at m/z 317 [$\text{M} + \text{H} - 2\text{H}_2\text{O}$]⁺ and its ^1H and ^{13}C NMR data (Table 1). Its molecular weight was 2 mass units higher than that of 10G, indicating that it might be the product from keto reduction of 10G. In addition to the distinguishable resonance for a methoxyl group (δ_{H} 3.77, 3H, s), its ^1H NMR spectrum (Table 1) also indicated the presence of a 1,3,4-trisubstituted phenyl group [δ_{H} 6.73 (1 H, $J = 8.0$ Hz); 6.61 (1 H, s); and 6.59 (1 H, d, $J = 8.0$ Hz)] and a methyl group (δ_{H} 0.78, 3H, t, $J = 7.0$ Hz). Its ^{13}C NMR spectrum (Table 1) displayed 21 carbon resonances, which were classified by HMQC experiments as two methyls, 11 methylenes, five methine, and three quaternary carbons. The aforementioned NMR data implied that the structure of this product was closely related to that of 10G. The only difference was its C-3 being assigned as an oxymethine (δ_{H} 3.88, 1H, m; δ_{C} 68.96) instead of the expected ketone carbonyl (δ_{C} 211.48) in 10G (Table 1). This was confirmed by the HMBC (Figure 3) correlations of H-1/C-3, H-2/C-3, and H-3/C-5. Therefore, we confirmed that it is the keto reduced product of 10G, [10]-gingerdiol. The other product showed molecular formula $\text{C}_{21}\text{H}_{36}\text{O}_4$ based on positive APCI-MS at m/z 317 [$\text{M} + \text{H} - 2\text{H}_2\text{O}$]⁺ and its ^1H and ^{13}C NMR data (Table 1). 2D NMR spectra (HMQC and HMBC) indicated that these two products possess the same planar structure (Figure 3). Since a new chiral center was formed, the difference between these two products arose at the configuration at C-3. After comparing the NMR data of these two products with those of the two known [6]-gingerdiols, (3*R*,5*S*)-gingerdiol and (3*S*,5*S*)-ginger-

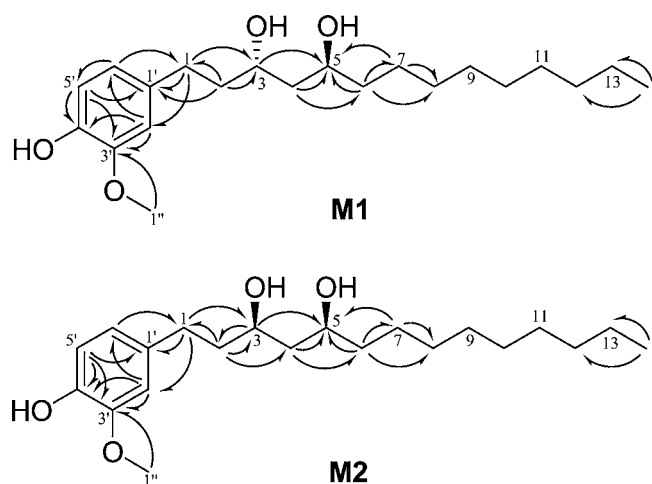


Figure 3. Significant HMBC (H → C) correlations of (3S,5S)-[10]-gingerdiol (M1) and (3R,5S)-[10]-gingerdiol (M2).

diol,^{20,21} we identified these two products as (3S,5S)-[10]-gingerdiol and (3R,5S)-[10]-gingerdiol, respectively.

Metabolites M1 and M2 showed the same retention times as those of the synthetic (3S,5S)-[10]-gingerdiol and (3R,5S)-[10]-gingerdiol, respectively, indicating that M1 and M2 were (3S,5S)-[10]-gingerdiol and (3R,5S)-[10]-gingerdiol, respectively. We further confirmed this by tandem mass spectrometry, which indicated that M1 and M2 had almost the same mass fragments as those of the synthetic (3S,5S)-[10]-gingerdiol and (3R,5S)-[10]-gingerdiol, respectively (Figure 4). Therefore, M1 and M2 were identified as (3S,5S)-[10]-gingerdiol and (3R,5S)-[10]-gingerdiol, respectively. Besides these two identified metabolites, there remains one unidentified metabolite at the retention time of 38.9 min (Figure 2D), for which we are unable to elucidate the structure at the current stage.

Metabolism of 10G in Human. While 10G was transformed into two isomeric metabolites, (3S,5S)-[10]-gingerdiol and (3R,5S)-[10]-gingerdiol, in zebrafish embryos, the metabolism of 10G in humans was still unclear. Thus, we

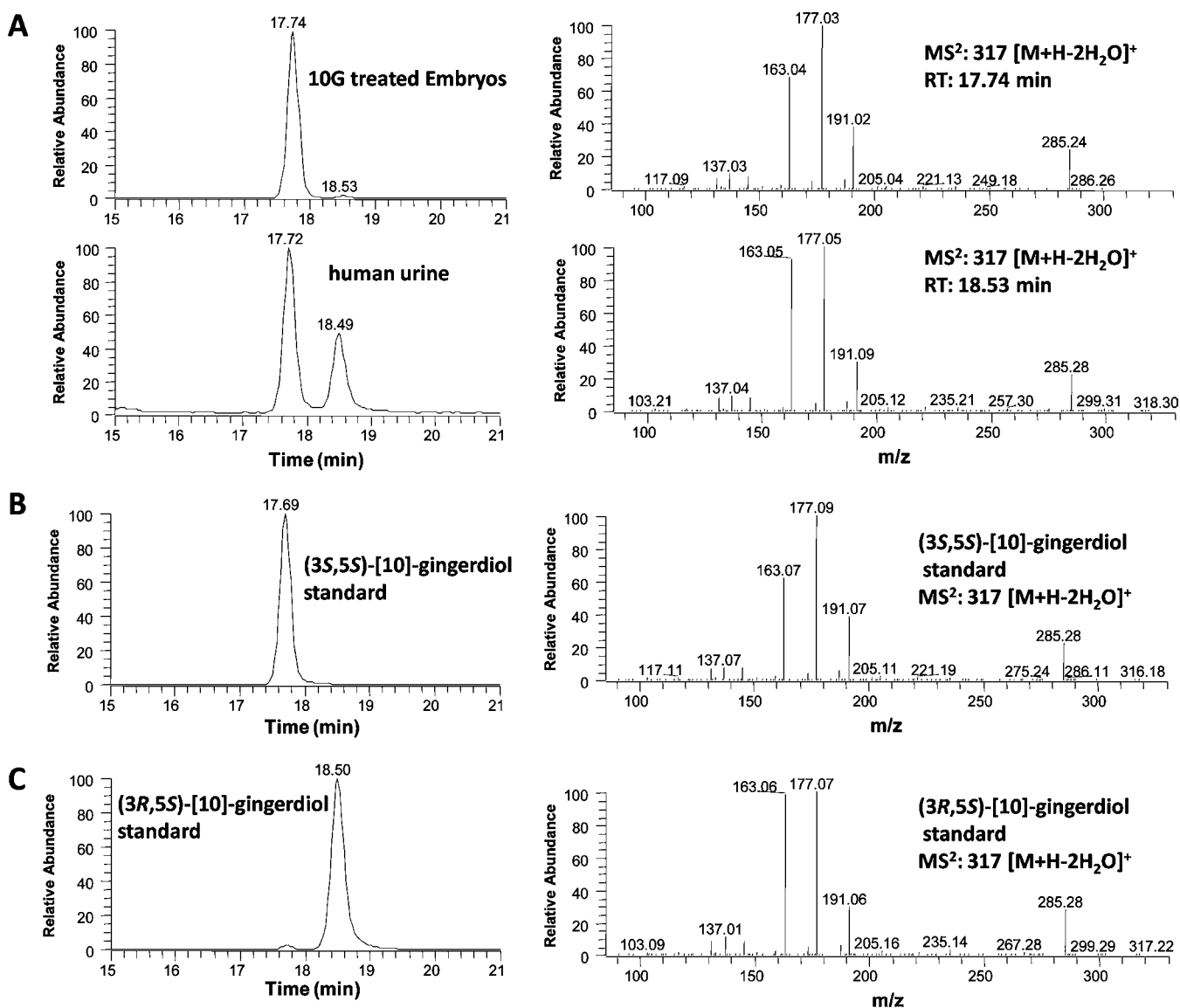


Figure 4. LC-MS² (positive ion) spectra of the lysate collected from [10]-gingerol (10G) treated zebrafish embryos and urinary sample collected from humans after drinking ginger tea (A). LC-MS² (positive ion) spectra of authentic (3S,5S)-[10]-gingerdiol (B) and (3R,5S)-[10]-gingerdiol (C).

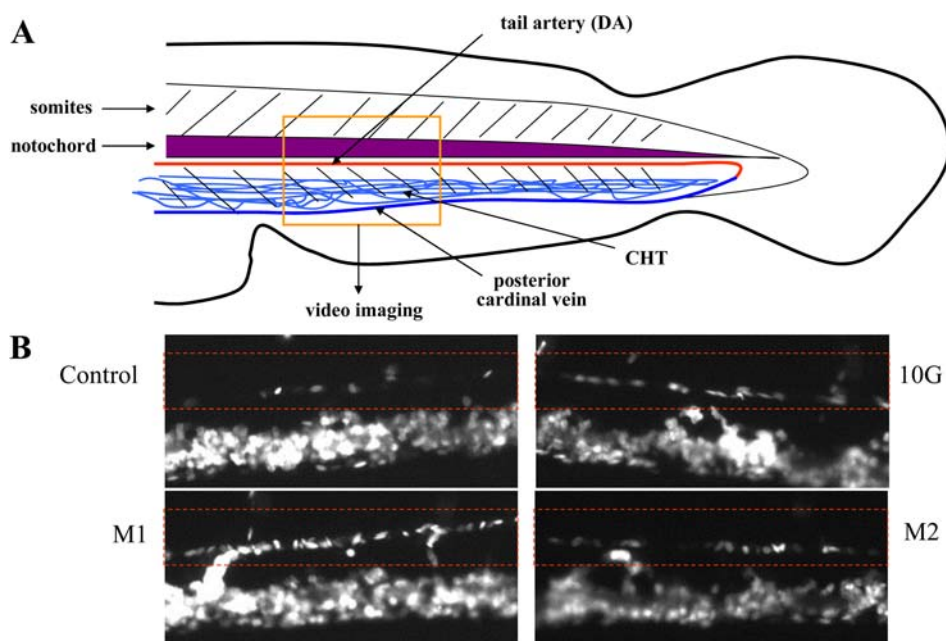
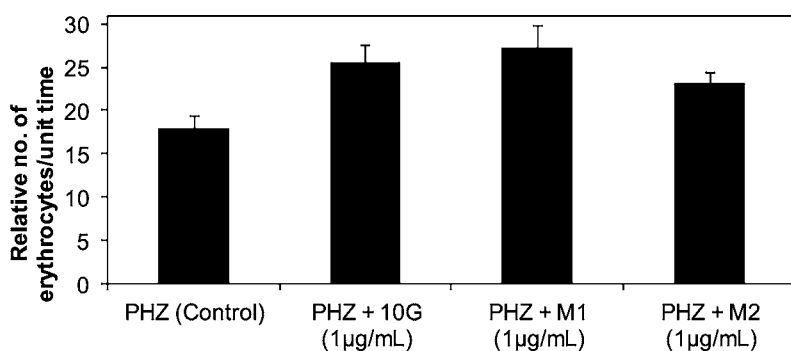


Figure 5. Chemical-induced anemia zebrafish model. A representative picture of zebrafish embryo showing the flow of erythrocytes in the dorsal aorta in the tail region (A). Representative fluorescent images of *Tg(gata1:dsRed)* for control, [10]-gingerol (10G), M1, and M2 (B). Red dashed rectangle indicates the flow of erythrocytes in the dorsal aorta.



	Blood Cells/Embryo	SEM	n	p value (vs CTL)
PHZ (Control)	17.93	1.44	30	
PHZ + 10G (1 µg/mL)	25.57	2.08	30	1.74E-03
PHZ + M1 (1 µg/mL)	27.16	2.75	24	1.19E-03
PHZ + M2 (1 µg/mL)	23.03	1.49	28	9.89E-03

Figure 6. Erythropoiesis-stimulating activity of [10]-gingerol (10G) and its metabolites M1 and M2 in zebrafish embryos. The relative number of erythrocytes was compared at 5 day postfertilization embryos during hematopoietic recovery after phenylhydrazine (PHZ)-induced anemia in zebrafish embryos. The relative number of erythrocytes is indicated as mean \pm SEM. *n* is number of embryos per group. *p* value from Student's *t* test.

pursued an experiment in which urine samples were collected from three healthy human subjects that were given ginger tea to drink. We then searched the urine samples for the two potential 10G metabolites, (3*S*,5*S*)-[10]-gingerdiol and (3*R*,5*S*)-[10]-gingerdiol, using LC/MS, and confirmed that 10G was extensively metabolized in humans in a similar manner as in zebrafish embryos, with the same major metabolites (Figure 4).

10G and Its Metabolites M1 and M2 Can Stimulate Erythropoiesis. We previously developed a chemical-induced anemia zebrafish model¹¹ in which zebrafish embryos developed acute hemolytic anemia and the condition was reversible. This model is feasible for testing the erythrocyte-

stimulating activity of compounds such as 10G and its metabolites M1 and M2 (Figure 5). Here we used PHZ to create acute anemia in zebrafish as the anemic control (17.93 ± 1.44). The addition of 10G promoted the production of erythrocytes during the hematopoietic recovery (25.57 ± 2.08 relative number of erythrocytes/unit time). In addition, both metabolites M1 and M2 exhibited a similar erythrocyte-stimulating activity in promoting the recovery from anemia condition, 27.16 ± 2.75 and 23.03 ± 1.49 relative number of erythrocytes/unit time, respectively (Figure 6). All 10G, M1, and M2 activities were higher than the control with statistical significance ($p < 0.01$).

DISCUSSION

Previously we reported that ginger extract and its purified components, especially 10G, potentially stimulated both the primitive and definitive waves of hematopoiesis in zebrafish embryos.¹¹ In order to clarify whether 10G itself or its converted metabolites showed this potent effect on hematopoiesis in zebrafish embryos, we first investigated metabolism of 10G in zebrafish embryos and then in humans upon the consumption of ginger tea containing 10G. Our results show that 10G is extensively metabolized in zebrafish embryos through a reductive pathway, and its two isomeric metabolites, (3S,5S)-[10]-gingerdiol (M1) and (3R,5S)-[10]-gingerdiol (M2), were identified by LC/MS analysis as well as comparison with synthesized standards. In addition, our results showed that 10G gives a similar metabolic profile in humans as it did in zebrafish embryos. That is, the two major reductive metabolites, (3S,5S)-[10]-gingerdiol and (3R,5S)-[10]-gingerdiol, were also found in human urine. To our knowledge, this is the first study on the metabolism of [10]-gingerol in zebrafish embryos and in humans.

Stereochemical configuration is a fundamental aspect of molecular structure. Substrate stereoselectivity may occur in enzyme-mediated catalysis by virtue of the innate asymmetry of the active site. Product stereoselectivity may also arise when new chiral centers are introduced during an enzymatic reaction, because enzymes may specifically stabilize only one of the possible transition states for a given reaction. In this study, we separated the diastereomers of [10]-gingerdiol to give the major metabolites. We observed that there were two dominant peaks (M1 and M2) in human urine compared to only one major peak (M1) in zebrafish embryos. We found that M1 had slightly higher activity in induction of erythropoiesis than M2, indicating that stereochemistry had some influence on biological efficacy. Additionally, M1 and M2 are the reducing products of ketone in 10G. It is reported that ketones can be reduced by carbonyl-reducing enzymes, which are grouped into two large protein superfamilies: the aldo-keto reductases (AKRs) and the short-chain dehydrogenases/reductases (SDRs).²² It is possible that the compositions of the carbonyl-reducing enzymes in zebrafish embryos and in humans are different, giving rise to the observed mismatched products. Substrate and product stereoselectivity by specific carbonyl-reducing enzymes remains to be fully explored, yet could help to further elucidate the biotransformation of 10G.

Erythropoiesis, the process by which red blood cells (erythrocytes) are produced, is conserved in humans, mice, and zebrafish.²³ Anemia is a common blood disorder and is characterized by a decreased number of erythrocytes, which we previously found that it would be abrogated by the treatment with 10G.¹¹ Both M1 and M2 had similar erythropoiesis-stimulating activity on zebrafish embryos as that of 10G, and M1 showed slightly higher activity than 10G. Our previous study confirmed that 10G could promote the expression of *gata1* in erythroid cells and increase the expression of hematopoietic progenitor markers *cmyb* and *scl*. We also demonstrated that 10G could promote hematopoietic recovery from acute hemolytic anemia in zebrafish. We displayed that 10G treatment during gastrulation resulted in an increase of *bmp2b* and *bmp7a* expression and their downstream effectors, *gata2* and *eve1*. At later stages 10G can induce *bmp2b/7a*, *cmyb*, *scl*, and *lmo2* expression in the caudal hematopoietic tissue. As

M1 and M2 display similar activity to 10G, it is likely that they exert their efficacies via this mechanistic pathway.

In conclusion, results from this study are important for understanding the metabolism of [10]-gingerol in zebrafish embryos and in humans and provide useful information that may act as a reference for nutraceutical developments toward treating anemia with ginger. Knowledge of the metabolism of 10G may help in understanding the mechanism of action and therapeutic effects of ginger extract in hematopoiesis. Even though studies have shown that zebrafish and mammals have common genetic pathways and regulators during hematopoiesis, whether ginger has the hematopoietic effect in human is a topic for future study.

AUTHOR INFORMATION

Corresponding Author

*Phone: 704-250-5710. Fax: 704-250-5709. E-mail: ssang@ncat.edu or shengminsang@yahoo.com.

Funding

This work was partially supported by grants CA138277 (S.S.) from the National Cancer Institute and CA138277S1 (S.S.) from National Cancer Institute and Office of Dietary Supplement of National Institutes of Health.

Notes

The authors declare no competing financial interest.

ABBREVIATIONS USED

10G, [10]-gingerol; APCI, atmospheric-pressure chemical ionization; hpf, hours postfertilization; HPLC, high-performance liquid chromatography; LC/MS, liquid chromatography/mass spectrometry

REFERENCES

- (1) Ali, B. H.; Blunden, G.; Tanira, M. O.; Nemmar, A. Some phytochemical, pharmacological and toxicological properties of ginger (*Zingiber officinale* Roscoe): a review of recent research. *Food Chem. Toxicol.* **2008**, *46*, 409–20.
- (2) Kubra, I. R.; Rao, L. J. An impression on current developments in the technology, chemistry, and biological activities of ginger (*Zingiber officinale* Roscoe). *Crit. Rev. Food Sci. Nutr.* **2012**, *52*, 651–88.
- (3) Zick, S. M.; Djuric, Z.; Ruffin, M. T.; Litzinger, A. J.; Normolle, D. P.; Alrawi, S.; Feng, M. R.; Brenner, D. E. Pharmacokinetics of 6-gingerol, 8-gingerol, 10-gingerol, and 6-shogaol and conjugate metabolites in healthy human subjects. *Cancer Epidemiol. Biomarkers Prev.* **2008**, *17*, 1930–6.
- (4) Masada, Y.; Inoue, T.; Hashimoto, K.; Fujioka, M.; Uchino, C. [Studies on the constituents of ginger (*Zingiber officinale* Roscoe) by GC-MS (author's transl)]. *Yakugaku Zasshi* **1974**, *94*, 735–8.
- (5) Yu, Y.; Huang, T.; Yang, B.; Liu, X.; Duan, G. Development of gas chromatography-mass spectrometry with microwave distillation and simultaneous solid-phase microextraction for rapid determination of volatile constituents in ginger. *J. Pharm. Biomed. Anal.* **2007**, *43*, 24–31.
- (6) Jiang, H.; Solyom, A. M.; Timmermann, B. N.; Gang, D. R. Characterization of gingerol-related compounds in ginger rhizome (*Zingiber officinale* Rosc.) by high-performance liquid chromatography/electrospray ionization mass spectrometry. *Rapid Commun. Mass Spectrom.* **2005**, *19*, 2957–64.
- (7) Kuhad, A.; Tirkey, N.; Pilkhwai, S.; Chopra, K. 6-Gingerol prevents cisplatin-induced acute renal failure in rats. *Biofactors* **2006**, *26*, 189–200.
- (8) Wu, H.; Hsieh, M. C.; Lo, C. Y.; Liu, C. B.; Sang, S.; Ho, C. T.; Pan, M. H. 6-Shogaol is more effective than 6-gingerol and curcumin in inhibiting 12-O-tetradecanoylphorbol 13-acetate-induced tumor promotion in mice. *Mol. Nutr. Food Res.* **2010**, *54*, 1296–306.

(9) Peng, F.; Tao, Q.; Wu, X.; Dou, H.; Spencer, S.; Mang, C.; Xu, L.; Sun, L.; Zhao, Y.; Li, H.; Zeng, S.; Liu, G.; Hao, X. Cytotoxic, cytoprotective and antioxidant effects of isolated phenolic compounds from fresh ginger. *Fitoterapia* **2012**, *83*, 568–85.

(10) Kim, J. S.; Lee, S. I.; Park, H. W.; Yang, J. H.; Shin, T. Y.; Kim, Y. C.; Baek, N. I.; Kim, S. H.; Choi, S. U.; Kwon, B. M.; Leem, K. H.; Jung, M. Y.; Kim, D. K. Cytotoxic components from the dried rhizomes of *Zingiber officinale* Roscoe. *Arch. Pharm. Res.* **2008**, *31*, 415–8.

(11) Ferri-Lagneau, K. F.; Moshal, K. S.; Grimes, M.; Zahora, B.; Lv, L.; Sang, S.; Leung, T. Ginger stimulates hematopoiesis via Bmp pathway in zebrafish. *PLoS One* **2012**, *7*, e39327.

(12) Yu, Y.; Zick, S.; Li, X.; Zou, P.; Wright, B.; Sun, D. Examination of the pharmacokinetics of active ingredients of ginger in humans. *AAPS J.* **2011**, *13*, 417–26.

(13) Wang, W.; Li, C. Y.; Wen, X. D.; Li, P.; Qi, L. W. Simultaneous determination of 6-gingerol, 8-gingerol, 10-gingerol and 6-shogaol in rat plasma by liquid chromatography-mass spectrometry: Application to pharmacokinetics. *J. Chromatogr., B: Anal. Technol. Biomed. Life Sci.* **2009**, *877*, 671–9.

(14) Zick, S. M.; Ruffin, M. T.; Djuric, Z.; Normolle, D.; Brenner, D. E. Quantitation of 6-, 8- and 10-gingerols and 6-shogaol in human plasma by high-performance liquid chromatography with electrochemical detection. *Int. J. Biomed. Sci.* **2010**, *6*, 233–240.

(15) Lewis DFV, L. B. Molecular modelling of members of hte P4502A subfamily: application to studies of enzyme specificity. *Xenobiotica* **1995**, *25*, 585–598.

(16) Sang, S.; Hong, J.; Wu, H.; Liu, J.; Yang, C. S.; Pan, M. H.; Badmaev, V.; Ho, C. T. Increased growth inhibitory effects on human cancer cells and anti-inflammatory potency of shogaols from *Zingiber officinale* relative to gingerols. *J. Agric. Food Chem.* **2009**, *57*, 10645–50.

(17) Shao, X.; Lv, L.; Parks, T.; Wu, H.; Ho, C. T.; Sang, S. Quantitative analysis of ginger components in commercial products using liquid chromatography with electrochemical array detection. *J. Agric. Food Chem.* **2010**, *58*, 12608–14.

(18) Chen, H.; Lv, L.; Soroka, D.; Warin, R. F.; Parks, T. A.; Hu, Y.; Zhu, Y.; Chen, X.; Sang, S. Metabolism of [6]-shogaol in mice and in cancer cells. *Drug Metab. Dispos.* **2012**, *40*, 742–53.

(19) Traver, D.; Paw, B. H.; Poss, K. D.; Penberthy, W. T.; Lin, S.; Zon, L. I. Transplantation and in vivo imaging of multilineage engraftment in zebrafish bloodless mutants. *Nat. Immunol.* **2003**, *4*, 1238–46.

(20) Lv, L.; Chen, H.; Soroka, D.; Chen, X.; Leung, T.; Sang, S. 6-Gingerdiols as the major metabolites of 6-gingerol in cancer cells and in mice and their cytotoxic effects on human cancer cells. *J. Agric. Food Chem.* **2012**, *60*, 11372–7.

(21) Kikuzaki, H.; Tsai, S.-M.; Nakatani, N. Gingerdiol related compounds from the rhizomes of *Zingiber officinale*. *Phytochemistry* **1992**, *31*, 1783–6.

(22) Oppermann, U. Carbonyl reductases: the complex relationships of mammalian carbonyl- and quinone-reducing enzymes and their role in physiology. *Annu. Rev. Pharmacol. Toxicol.* **2007**, *47*, 293–322.

(23) Palis, J.; Segel, G. B. Developmental biology of erythropoiesis. *Blood Rev.* **1998**, *12*, 106–14.